The 14th International Topical Meeting on Nuclear Reactor Thermalhydraulics, NURETH-14
Toronto, Ontario, Canada, September 25-30, 2011

NURETH14-060

ANALYSES OF LIGHT GAS STRATIFICATION EROSION AND BREAK-UP UNDER THE EFFECT OF A VERTICAL JET: CFD SIMULATIONS FOR A COMMON TEST IN THE PANDA AND MISTRA FACILITIES

M. Sharabi and M. Andreani
Paul Scherrer Institut, CH-5232 Villigen, Switzerland

Abstract

Accurate predictions of thermal-hydraulic phenomena in nuclear reactor containments are highly required for safety assessment and for the design of accident mitigating measures. In the present work, the results obtained by the GOTHIC and FLUENT CFD codes are compared with the experimental data of a common test conducted in the PANDA and MISTRA test facilities. The initial condition of the test describes a stratified environment, where a layer of helium-rich mixture is produced in the upper part of one vessel, which is eroded by air injection from below. The ability of both codes to reproduce the observed phenomena is discussed in terms of comparisons with helium distributions and the air plume penetration velocity.

Introduction

The accurate prediction of gas mixing and transport in nuclear reactor containments is necessary for safety assessment and for the design of accident mitigation measures in the case of a severe accident with release of hydrogen. The evaluation of the capability of the codes used for containment safety analysis to simulate these phenomena is thus the object of intense research, which aims at providing information on merits and limitations of the various classes of codes (Lumped-Parameter codes, dedicated containment codes, commercial CFD codes), and on their range of applicability [1]. In particular, the interaction of rising jets or plumes with a layer of light gas accumulated at the top of a volume, and the associated processes of stratification break-up or gradual erosion of this layer is one of the focal points of the current research. Indeed, one of the most noticeable results of the International Standard Problem 47 [2] was that CFD codes could not reproduce the disruption of the stratified conditions caused by the injection of pure steam following a period of helium injection. Some simulations using Lumped Parameter (LP) codes could predict the phenomenon, but their success depended on the nodalisation used and the associated entrainment. Therefore, it became obvious that further research was needed to clarify to what extent the results are affected by the mesh used and if improved models (especially for turbulence) are required to simulate the complex flow conditions resulting from the formation of a negatively buoyant plume at the density interface [3]. In order to understand the root of the observed difficulties of the codes, experiments with simplified configurations and boundary conditions were also recommended.

One of the experimental programs dedicated to the general investigation of stratification break-up due to mass and energy sources or sinks is the recently concluded OECD SETH-2 project [4]. One of the test series performed in both MISTRA and PANDA facilities within this project included various tests with injection of fluid from below a layer of helium-rich mixture. Among these tests, a fundamental “common test” was defined for both facilities, where air and helium were used as working fluids instead of steam and helium, to avoid the complications associated with natural convection flows produced by heat transfer with the structures, which necessarily present for a steam-gas system.

Some results obtained with the GOTHIC code [5] with an axis-symmetric model for tests in PANDA for the configuration with central injection [6] indicated that a sufficiently fine mesh was necessary to obtain reasonable results for the speed of erosion of the upper layer. These results, however, also indicated that the turbulence model was critical for obtaining more accurate predictions. As the GOTHIC code has a very limited selection of turbulence models and can be efficiently used only with a coarse mesh, it became necessary to use a commercial CFD code to investigate in more detail the two issues of the effect of the mesh in the more general situation requiring a 3-D representation of the fluid domain and of the choice of the turbulence model. Due to the fundamental nature of the study, it was decided to first evaluate the capability of a CFD approach using the data of the “common test” with air and helium. This work reports on the initial investigations, which provide information on the gain in accuracy that can be obtained using a fine mesh. In future works, the role played by the modeling of turbulence will be discussed.

1. Description of the facilities

1.1. MISTRA facility

The MISTRA facility, located at CEA France and schematically shown in Figure 1a, consists of a stainless steel vessel, thermally insulated from the outside environment with a 20 cm thick layer of rock wool. The facility is used for containment thermalhydraulics and hydrogen risk studies. The vessel has an internal diameter of 4.25 m and a height of 7.38 m, giving a free volume of 97.6 m^3, and comprises two shells, a flat head and a curved bottom. The facility accommodates an inner cylinder of 1.906 m diameter and a ring plate welded to its circumference. Three condensers are included in the containment and installed with gap from the wall; each with a regulating circuit to control the wall temperature and hereby enable reproducing representative accidental conditions of PWR containments. A vent of 0.2 m diameter is located at an elevation of 1.9 m to allow for a constant pressure test. Different injection geometries are allowed in the facility. Radial injections are available at four points at a height of 6.559 m. These lateral injection lines are distributed symmetrically around the vessel axis to provide axisymmetric distribution of the stratification during test initialization. For the test considered in the present study, vertical injection is provided at an off-centered location from a pipe (chimney) which protrudes from the ring plate. The pipe is at 1.35 m from the axis and its diameter is 72 mm. More details about the MISTRA facility can be found in [7].

1.2. PANDA facility

The PANDA is an integral, multicompartment large scale facility, located at Paul Scherrer Institut in Switzerland, which has been recently used also for investigating containment related phenomena of Light Water Reactors, i.e. for separate-effect tests. The facility consists of six cylindrical vessels representing relevant components of advanced LWRs: reactor vessel, gravity driven cooling system, dry- and wet-wells (each represented by two identical vessels with interconnecting tubes). The vessels make a total volume of 460 m^3. For the test investigated in the present work, only part of the PANDA facility is used; this is the drywell vessels. The two vessels (Vessel 1 and 2) are connected by a pipe of 1 m diameter (see Figure 1b). There is one vent to outside installed at the top of Vessel 2 with the aim to keep the pressure constant when it is opened. The dry well vessels are 8 m height and 4 m diameter, giving a volume of 180 m^3. An injection pipe is installed in Vessel 1 for near-wall injection with its center line situated at a distance 0.5 m from the wall (1.5 m form the axis) and opposite to the interconnecting pipe. The diameter of the injection pipe is 75 mm. A helium rich layer at the top of the vessel can be created using a pipe of diameter 58 mm at elevation 6 m and inclined upward at 5^o from the horizontal. More details about the PANDA facility can be found in [8].

2. Test description

The facilities use helium as a simulant gas for hydrogen for investigation of light gas stratification and erosion phenomena. The common test aims to compare both facilities for similar test conditions in order to assess the effect of the different geometry for the interaction of an air jet with a stagnant helium rich layer. The test performed in both facilities describes a stratified environment, where a layer of helium-rich mixture (~40% helium and ~60 % air) is produced at the upper part of one vessel, the lower part for the same vessel (and the second vessel in PANDA) being filled with pure air. This represents the initial conditions of stratification before the initiation of the test. Table 1 summarizes the initial and boundary conditions designed for the test in PANDA (ST1_7)[1] and MISTRA (LOWMA) facilities. Air is injected from below at different mass flow rates to erode the helium rich layer. Both facilities are open to the atmosphere through vents to allow for a constant pressure test.

The ability of the air jet to erode the stratified helium layer can be described by an interaction Froude number [3] defined by:

$$Fr = U / NL \tag{1}$$

where U is the local velocity at the interface, which is calculated from [3]:

$$U = 6.2 U_{inj} \frac{d_{inj}}{\left(z - H_{inj}\right)} \tag{2}$$

being z the elevation of the bottom of the helium-rich layer and L the full width of the air jet at the helium cloud, this is calculated from:

$$L = 0.172(z - H_{inj}) \tag{3}$$

The characteristic pulsation of the stratification is defined as:

---

1 This experiment was repeated twice, with velocity measurements being performed during the second test ST1_7_2. Therefore, most comparisons are performed with this repeated test.

$$N = \sqrt{\frac{2g(\rho_{air} - \rho_s)}{(\rho_{air} + \rho_s)\Delta z}} \tag{4}$$

Δz in the above equation refers to the approximate vertical length where the helium concentration difference occurs. If the interaction Froude number is greater than one, the flow is dominated by the momentum of the air jet leading to penetration of the helium layer. LOWMA3 test in MISTRA facility is designed to have an interaction Froude number of 1 at the start of the test, while LOWMA4 is represented by a higher mass flow of the injected air and is dominated by momentum effects. Different test parameters are given in Table 2. ST1_7 has the highest Froude number due to the shorter distance between the source and the density interface but due to the larger helium reservoir in the top of the PANDA vessel, the penetration of the air jet can be slower than in LOWMA4.

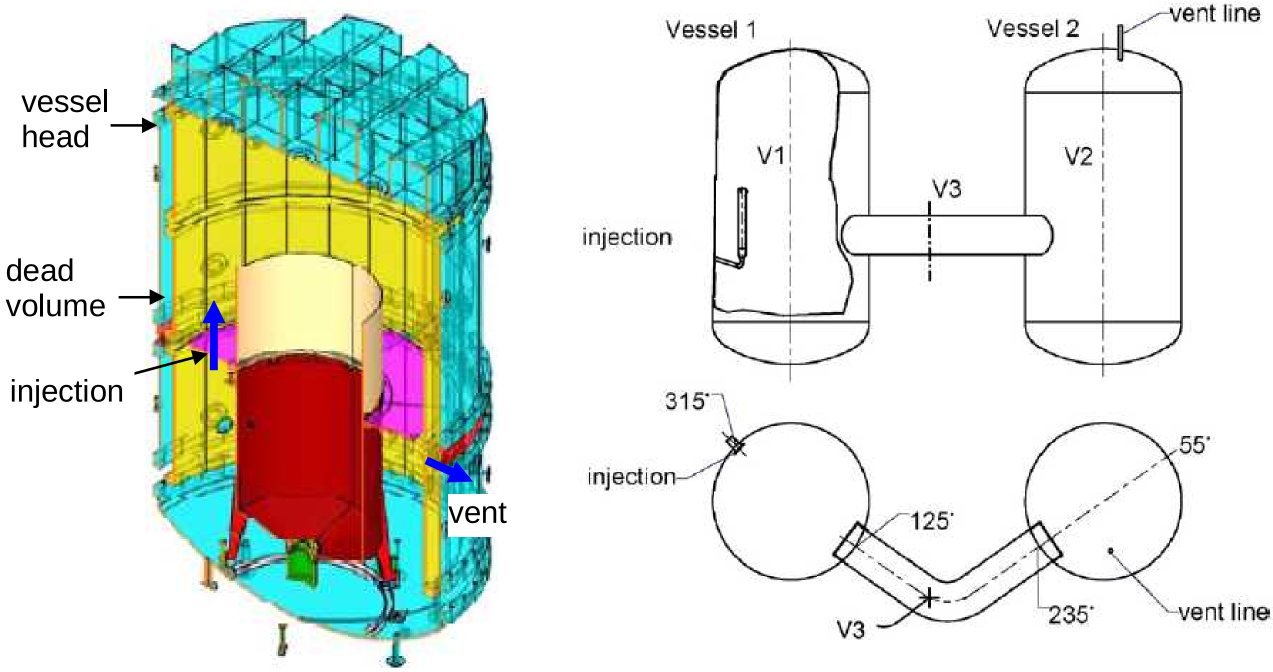

(a) MISTRA facility (b) PANDA facility

Figure 1 Schematics of test facilities.

The concentration measurements considered in this work are obtained using mass spectrometry for PANDA and mini-katarometers for MISTRA. The sensors in the PANDA facility are located at a vertical plane passing through the injection axis and are arranged in vertical lines at different distances from the vessel axis. In MISTRA case, on the other hand, the sensors are arranged in the following way (considering azimuthal and radial coordinates):

- For sensors TCG0 to TCG9, 157.5^o from the injection axis and radius = 1.54 m
- For sensors TCG10 to TCG19, 112.5^o from the injection and radius = 1.06 m
- For sensors TCG20 to TCG29, 21^o from the injection and radius = 1.48 m

In addition, velocity measurements are performed using particle image velocimetry (PIV) in the PANDA test at the vessel symmetry plane passing through the jet axis.

Table 1 Initial and boundary conditions for PANDA and MISTRA tests.

Parameter	PANDA (ST1_7)	MISTRA (LOWMA)
Injection diameter, d_{inj}	75 mm	72 mm
Injection height, H_{inj}	4013 mm	3660 mm
Initial pressure	0.974	1.005 bar
Initial temperature	288 K	292 K
Injected air temperature	303 K	292 K

Table 2 Test description parameters for PANDA and MISTRA facilities.

Test	$\dot{m}_{air}$ (g/s)	U_{inj} *(m/s)*	z (m)	*Fr*
PANDA ST1_7	15.02	3.03	0.86	6.04
MISTRA LOWMA3	15.17	3.11	2.14	1.0
MISTRA LOWMA4	50.58	10.36	2.14	3.35

3. Numerical methods

3.1. CFD calculations

The FLUENT CFD 6.3 [9] commercial code is used in the CFD simulations reported in the present paper. The computational domain and the mesh layout for both facilities are shown in Figure (2).

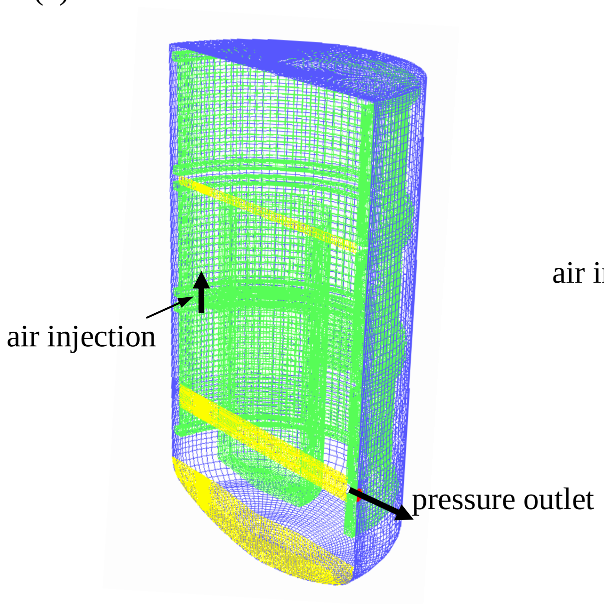

(a) MISTRA

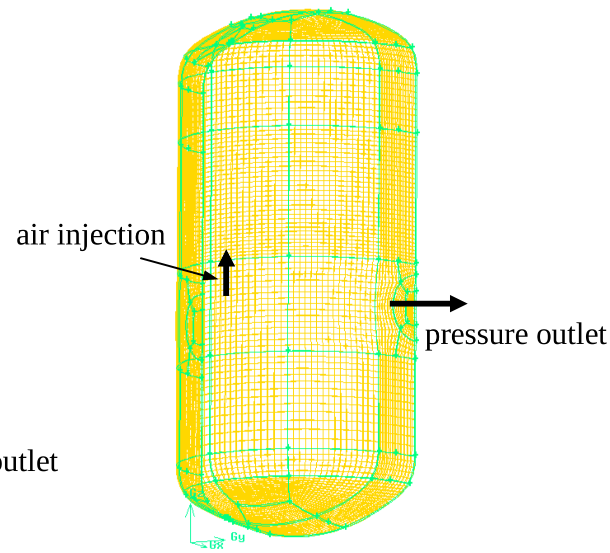

(b) PANDA

Figure 2 Mesh layouts for the CFD calculations (a) MISTRA (b) PANDA.

To economize on the number of cells and the CPU time, only half of the MISTRA vessel is considered in the simulation assuming symmetry boundary conditions at the plane passing through the axis of the jet. For the PANDA facility, the second vessel is not considered and only half of vessel 1 is simulated. Actually, the intersection of the interconnecting pipe is not divided symmetrically around the vessel symmetry plane, though symmetry is assumed to simplify the geometry. Atmospheric pressure is assumed at the vessel outlet as a boundary condition. These assumptions will have only little influence on the helium distribution in vessel 1 of PANDA. Flat velocity profiles are assumed at the source with a turbulent intensity of 4%. The initial conditions of helium distribution, shown in Figure 3, are given to the code at the start of the calculations.

Blocked fully structured hexahedral elements are adopted to mesh both facilities using about 400k grid points for MISTRA and 220k grid points for PANDA. High density of mesh cells are constructed around the injection source. Mesh sensitivity study is conducted for MISTRA to check the independence of the results on the size of the mesh employed.

Two turbulent models are used in the simulations performed in the present study: the standard k-ε model [10] and the RNG k-ε model [11], each employing the standard wall functions. Second order upwind differencing scheme is employed for discretization of the convective terms in the momentum, turbulence and species transport equations. The PRESTO (PREssure Staggering Option) scheme [9] is used for pressure interpolation. The PRESTO interpolation is suggested for situations where steep pressure gradients are encountered. This scheme performs continuity balance over a staggered control volume for each face to calculate the face pressure, inspiring the idea of staggered grid method used to avoid checkboard instabilities [12]. Standard linear interpolation instead, results in significant mass errors around the density interface showing spurious velocity fields and incorrectly high mixing rates.

Pressure velocity coupling is based on the PISO algorithm [13]. First order fully implicit backward time differencing is used in conjunction with the adaptive time stepping algorithm (the time step is varied between 0.02 and 1 second during the calculations based on the truncation error associated with the time integration). Convergence tolerance is set to 10^{-6} for momentum and turbulence equations and to 10^{-8} for species transport equation.

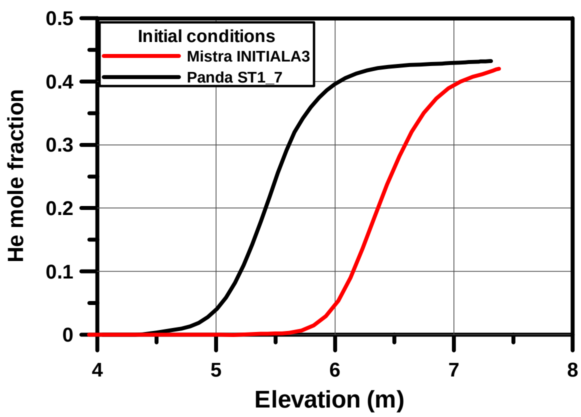

Figure 3 Helium distributions at the beginning of the test in PANDA and MISTRA.

3.2. GOTHIC calculations

GOTHIC [5] is a general-purpose, thermal-hydraulics computer program for design, licensing, safety and operation analysis of Nuclear Power Plant (NPP) containments and other confinement buildings. The thermal-hydraulics module is based on a two-phase, multi-fluid formulation, and solves separate conservation equations for mass, momentum and energy for three fields: a multi-component gas mixture, a continuous liquid, and droplets. In addition, species balances are solved for each component of the gas mixture. GOTHIC includes a full treatment of the momentum transport terms in multi-dimensional models, with optional models for turbulent shear, and for turbulent mass and energy diffusion. The options for turbulence are the mixing-length model and several variants of the k-ε model. The hydraulic model of GOTHIC is based on a network of computational volumes (one, two or three-dimensional) connected by flow paths. In contrast to standard CFD packages, in GOTHIC the subdivision of a volume into a multi-dimensional grid is based on orthogonal co-ordinates. The actual geometry of volumes with curved surfaces (e.g., a cylindrical vessel) can be represented, however, by blocking groups of cells. The numerical solution of the transport equations is based on a semi-implicit method. The method is first-order in time, whereas for the space-discretisation of the advection term both a first-order upwind and a bounded second-order method are available. The version of the code used in the present analysis is GOTHIC 7.2b. The standard GOTHIC high-Reynolds number k-ε model has been used to represent turbulence and the second-order method in space has been selected.

The nodalisations used for the simulations of the tests in the two facilities are shown in Fig. 4, where the inset also shows the detail of the mesh in the region of the injection tube. For both models the same meshing approach has been adopted, which consists of representing the pipe cross section with only one partly blocked square cell, with size equal to the diameter of the pipe. For both nodalisations, the vertical size of the cells above the injection is approximately equal to the length in the other two directions. This approach, which permits to minimize the momentum loss in the first cell above the injection, has been applied to all previous 3-D investigations carried out by the authors with GOTHIC [6, 14].

4. Results and discussions

Validations of the calculation results obtained by CFD FLUENT calculations and by the GOTHIC code are illustrated in terms of comparisons with experimental data for helium molar fraction distributions at different elevations and also for the velocity field which is available for the PANDA test ST1_7.

4.1. Helium distributions

Initially, full three dimensional turbulent calculations are performed for the pure diffusion test INITIALA3 conducted in the MISTRA facility which involves no air injection. It is important to verify that the numerical model is able to reproduce this reference test before considering the intervention of complicated phenomena. In this study, comparisons of results from the MISTRA tests are made only with data from the measuring locations TCG20-29. Data from other measuring locations were obtained for slightly different boundary conditions of the repeat tests and will not be considered here. Also, it was found from experimental data (using mass spectrometry) not shown here that the distribution of helium is almost axisymmetric. Figure 5 shows the comparisons of helium distribution obtained by CFD calculations at different elevations for a time span of 6000 s. The initial conditions are similar to those in Figure 3. The obtained results show the diffusion of helium from the upper levels in the vessel to the lower ones is in very good quantitative agreement with the experimental observations. Similarly good results were also obtained with the GOTHIC code.

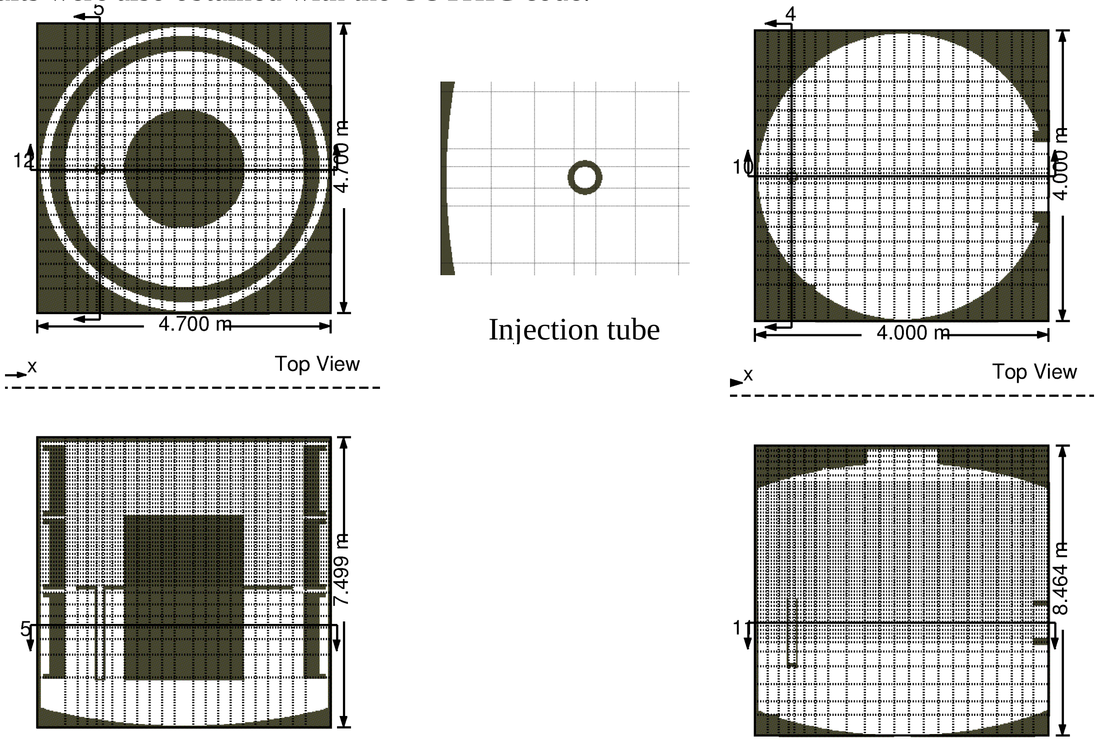

a) MISTRA b) PANDA

Figure 4 Nodalisations used for the simulations with GOTHIC: a) MISTRA; b) PANDA.

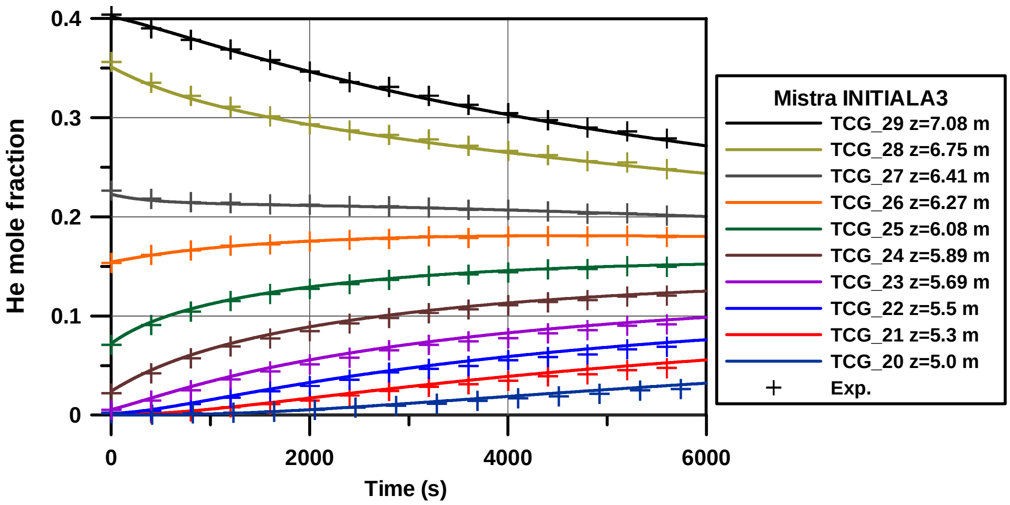

Figure 5 Comparison of helium distributions using the FLUENT code for the pure diffusion test in the MISTRA facility.

Next, the MISTRA test LOWMA3 is simulated with the FLUENT CFD code and the GOTHIC containment code using the standard k-ε turbulence model. The results obtained by both simulations are depicted in Figure 6 along with the experimental data. In the FLUENT simulations, the concentration time history at the elevation of TCG29 is well reproduced for up to 2000 s and the level of TCG28 for about 1000 s. This behavior is observed for the time period when the process is governed by pure diffusion. However, the predictions deviate significantly from the experimental data when the influence of the jet starts to impact the upper layers. At the intermediate elevations instead, high deviations are observed since the beginning of the test.

The predictions with GOTHIC also show a similar trend, the concentrations at the higher elevations being well predicted at the beginning and the calculations at all levels increasingly deviating from the experiment later in the transient. The results are in general closer to the measured data than those obtained with FLUENT, but they strongly depend on the choice of the mesh close to the injection. It will be reported in a future work that by increasing the cell size it has been possible to reproduce the experimental results at some elevations nearly perfectly. It would be therefore incorrect to conclude from Figure 6 that the predictive capability of a coarse mesh model is superior to that of a model using a fine mesh.

Sensitivity analyses of the results obtained by the FLUENT code for the first 1000 s are shown in the next figures. In Figure 7, comparisons of the results obtained using first and second order Upwind schemes are illustrated showing very little difference between the two differencing method indicating good accuracy of the grid used. Grid resolution is also checked using a mesh twice denser in the axial direction, in the region starting from the source to the top of the vessel. The obtained results are shown in Figure 8 showing only slight differences to the results in Figure 7 for the elevation TCG26. This is the elevation where the jet velocity reaches zero as will be demonstrated in the next subsection. The results obtained using the RNG k-ε model are shown in Figure 9 with almost no difference with the results shown in Figure 8 obtained using the standard k-ε turbulence model. Possible reasons for deficiencies in reproducing the experimental data by the FLUENT code can be attributed to the modeling of turbulence production/destruction which is based on the simplified gradient hypothesis [15]. This may underestimate the turbulence level in the areas of jet interactions and will be further investigated in a future work.

The results of the simulations for the ST1_7 by the FLUENT and GOTHIC codes are shown in Figures 10 and 11; for the vessel and injection pipe axes, respectively. The general trends of helium distributions are well captured by the codes. The upper layer are dominated by pure diffusion and not affected by the impact of the jet for the test duration shown in the figures. Comparing figures 10 and 11 for the same elevations, it can be found that the distributions do not change significantly at different radial locations. However, faster dilution takes place at lower elevations as the air jet penetrates inside the helium layers. This is clear for the G elevation in both figures. In both simulations and the experimental data, the helium molar fractions reach the same homogenized value ~8%. Only for the elevation I, the FLUENT calculation deviates from the experimental data. This can be attributed to the omission of the second vessel from the simulation and the reversed air flow at the pressure outlet (in the experiment, a mixture of air and helium instead may re-enter Vessel 1). This effect should actually be captured by the GOTHIC model (which includes both vessels), but it is likely be missed because of the coarse mesh used.

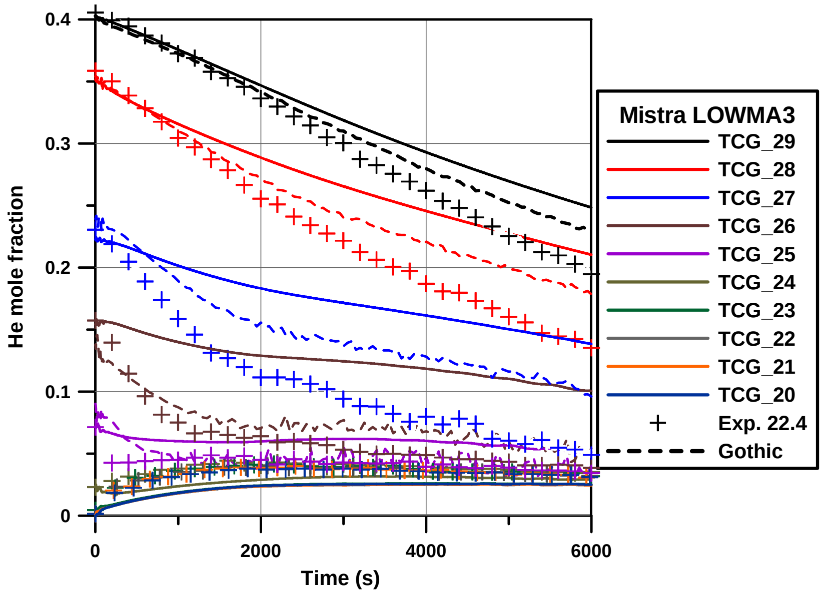

Figure 6 LOWMA3 simulation results by FLUENT and GOTHIC codes.

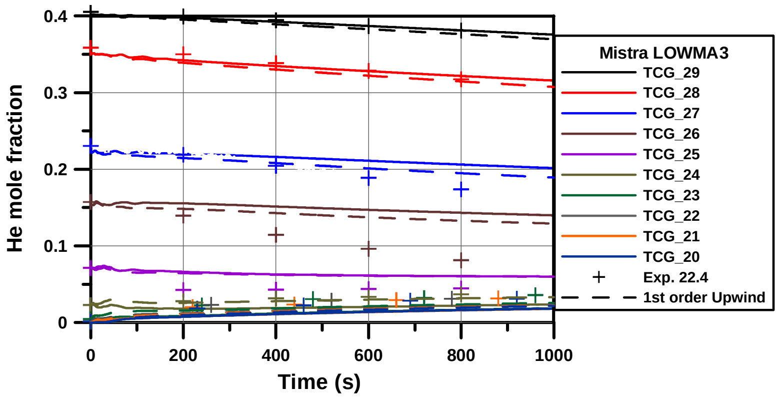

Figure 7 LOWMA 3 simulation results using 1st and 2nd order upwind differencing.

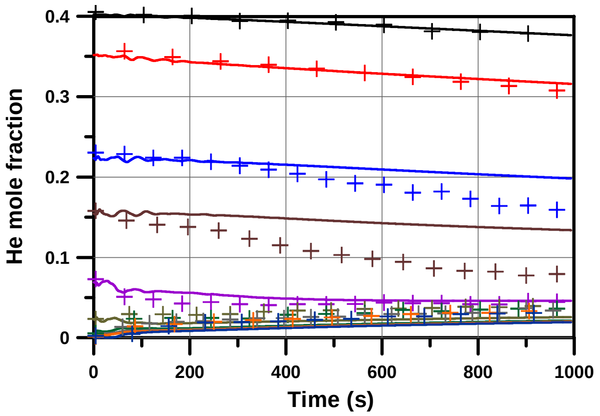

Figure 8 Simulation results obtained using a denser grid in the axial direction (LOWMA3). (see the legend in Figure 7)

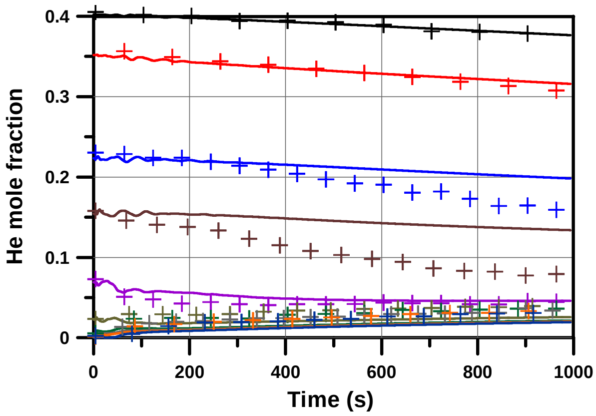

Figure 9 Simulation results obtained using the RNG k-ε model (LOWMA3). (see the legend in Figure 7)

As for the test LOWMA3, the calculation with GOTHIC may appear closer to the measured data than those obtained with FLUENT, However, a closer look at the trends in the curves, especially levels D, F and G, reveal that sudden drops are predicted at the beginning of the transient and the gradual change in the slope moving from one level to the next is not reproduced. It is clear that the process of gradual erosion is not well predicted. Moreover, as for LOWMA3, an increase of the size of the cell close to the injection resulted in a much faster progression of the upwards penetration of the jet. However, this time the speed of the erosion process was strongly overpredicted. These parametric studies, which show the sensitivity of the results obtained with the coarse-mesh approach to the nodalisation and the case-by-case effect of the cell size on the quality of the results, will be reported in a future work.

In LOWMA4 the mass flow rate of the injected air is increased to 50 g/s giving a Froude number of 3.35. Although the Froude number in LOWMA4 is lower than ST1_7, faster break-up and dilution of the whole stratified layer took place in LOWMA4. This is due to the larger helium reservoir in the top of the vessel 1 in the PANDA test.

The results of simulations obtained by the FLUENT code in comparison with the experimental data are shown in Figure 12. It is noted for this test in the MISTRA facility that the trends are qualitatively reproduced by the simulations. The upper layer is initially governed by molecular diffusion and the nearly constant concentration of the first 100 s is well captured in the simulation, but later there is a delay of about 50 s in the simulations to respond to the impact of the jet. Nevertheless, both the experiment and the simulation predict the same homogeneous helium concentration value after 300 s and the process of sequence dilution of helium layers with the development of time is reproduced by the calculations.

4.2. Velocity distributions

The velocity field in the plane of the injection gives more insight on the mechanism of erosion of the stratified layer. The discussion in this section is based on the results obtained by the FLUENT code. First, the axial velocity component is compared against the experimental data available from ST1_7 of the PANDA facility. Figure 13 shows these comparisons at different test times and in addition, for reference purposes, the distribution of the free jet velocity calculated from Equation 2 is shown for the same test conditions. It can be seen from the figure that velocity distributions predicted by the code follow very well the free jet distribution up to a certain height and then deviate due to the resistance encountered from the helium layer. The results obtained for ST1_7 compare reasonably well with the experimental data and the locations where the maximum centerline velocity reaches zero are well captured by the code. Similar plots for LOWMA3 are shown in the same figure, however without experimental data being available. It can be observed from the figure that, while jet penetrates the stratified layer in the case of ST1_7 with progression of time, the jet loses its momentum at the density interface in LOWMA3, according to the calculated results, and does not penetrate inside the stratified layer leading to thickening of the interface.

Further insight on the erosion process can be achieved from the velocity vectors and comparisons with the experimental data available from ST1_7. Figure 14 shows the velocity vectors for ST1_7 (at two different times) in qualitative comparisons with the data available from the PANDA test. The trends are well predicted by the simulation in terms of maximum velocity, spreading of the jet and location of the zero velocity. The helium layer is eroded due to entrainment into the lower layers by the action of two vortices. The corresponding helium contours are also shown in the figure demonstrating the motion of the interface and the dilution of the stratification with progression of time.

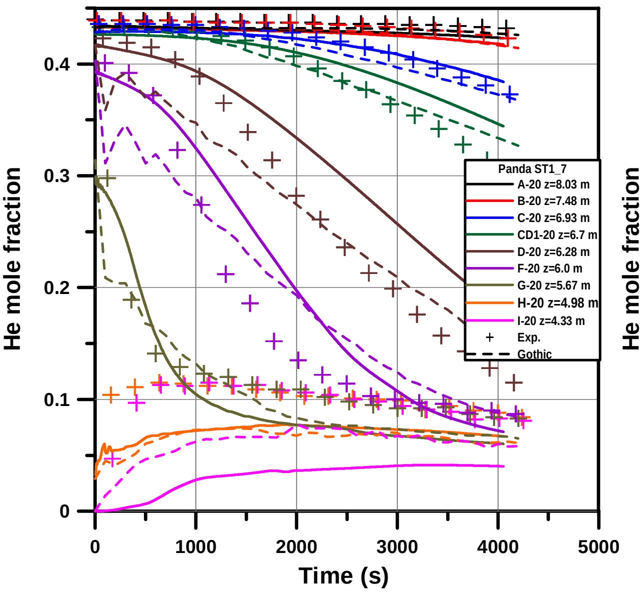

Figure 10 Helium distributions at the vessel axis for ST1_7 by FLUENT and GOTHIC.

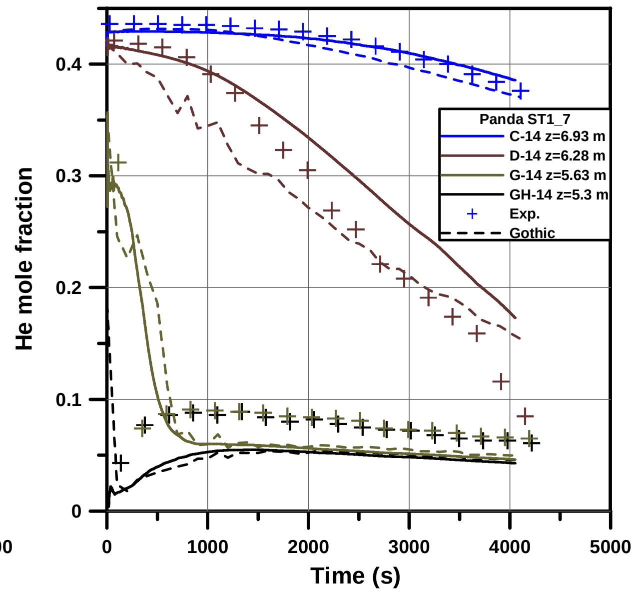

Figure 11 Helium distributions at the injection axis for ST1_7 by FLUENT and GOTHIC.

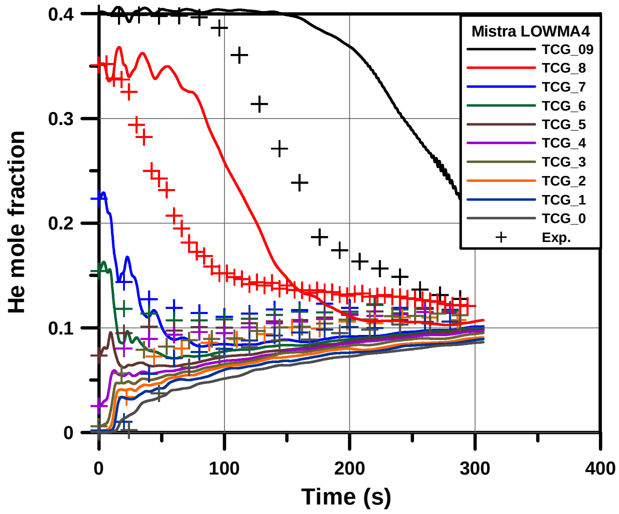

Figure 12 Helium distributions for LOWMA4 obtained by the FLUENT code.

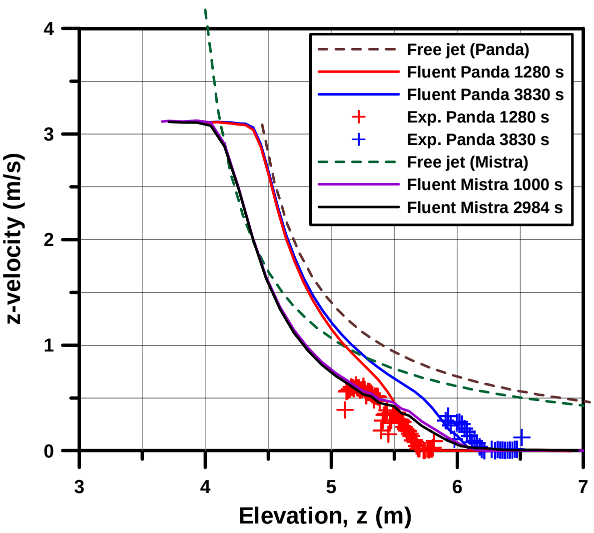

Figure 13 Velocity distributions at injection axis for ST1_7 and LOWMA3.

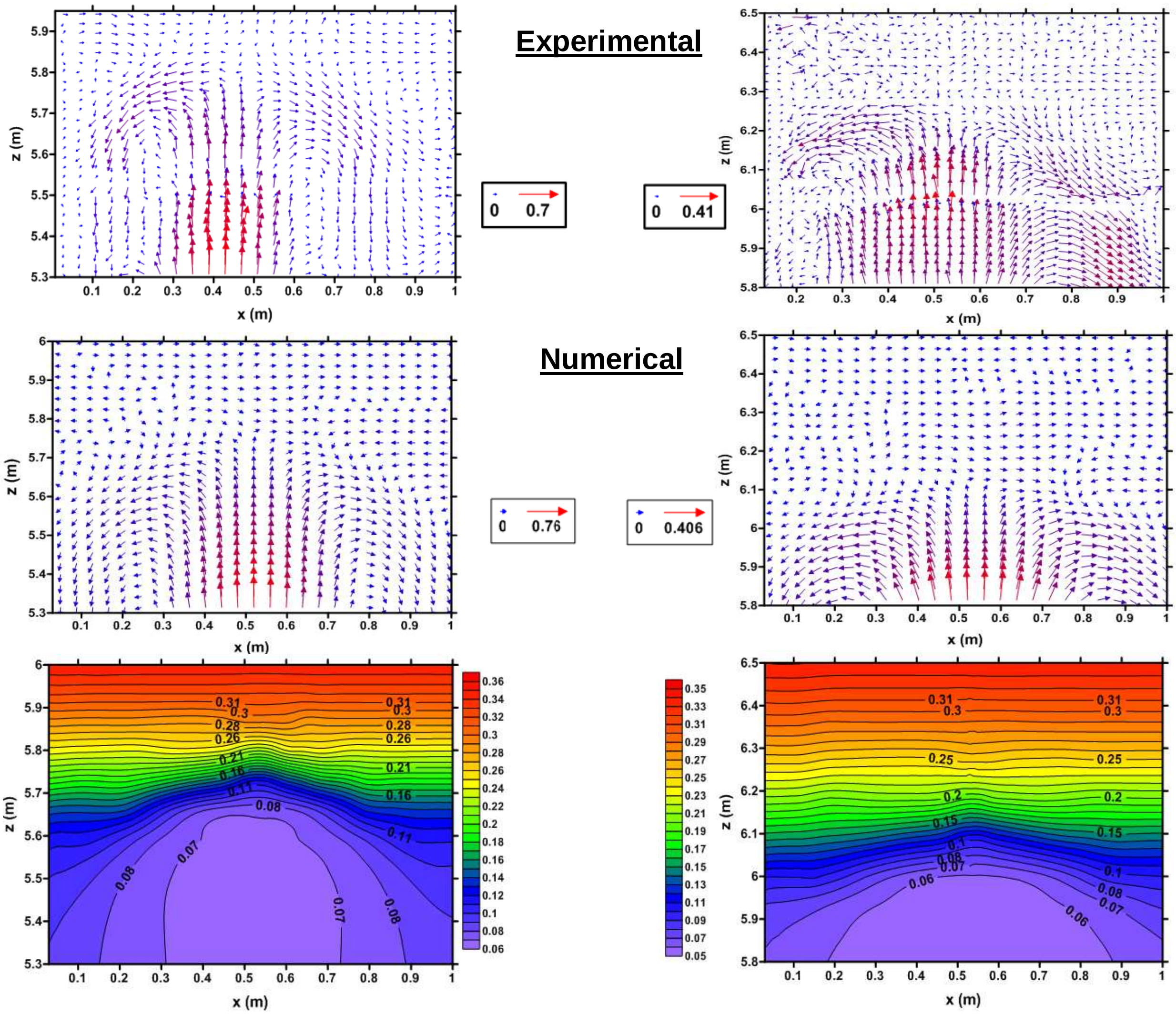

(a) t = 1280 s (b) t = 3830 s

Figure 14 velocity vectors and concentration contours at the injection plane for ST1_7.

5. Conclusions

Simulations of erosion of a helium rich layer by a vertical air jet are performed using FLUENT CFD and GOTHIC codes for tests conducted in PANDA and MISTRA facilities imposing different air flow rates and interaction Froude numbers. The calculations for the pure diffusion tests reproduced well the experimental data by full three-dimensional turbulent calculations showing the capability of the adopted models to reproduce this reference case.

For the common test conditions (ST1_7 and LOWMA3), the results obtained for the PANDA ST1_7 (*Fr*>1) test showed the erosion of the stratified layer and the entrainment of helium from the upper layer by the impact of the jet in a reasonably good agreement with the data in terms of helium and velocity distributions. On the other hand, the FLUENT results for the LOWMA3 test (with *Fr*=1) test showed large deviations, especially at intermediate elevations influenced by the jet. Sensitivity analyses showed independence of the obtained results on the density of the mesh used, spatial discretization and two adopted turbulence models. Further analyses in future work will be considered especially for modeling of the turbulence production due to buoyancy.

The high mass flow rate test, LOWMA4 (*Fr*>1), was also reasonably reproduced by the FLUENT calculations showing the differences between LOWMA3 and LOWMA4 for erosion and thickening of the interface in the first and progressive dilution of the stratified layers in the second.

The calculations with GOTHIC with a coarse mesh showed that using the appropriate nodalisation (developed on the base of the experience) it is possible to obtain results of the same quality as those obtained using a CFD code and a much finer mesh. However, the sensitivity of the results to the cell size close to the injection, and the observation that for one of the two tests a modification to the "expert" mesh is required to obtain reasonably good predictions, poses some question on the reliability of calculations for new conditions, when it is not possible to decide whether a correction to the standard approach will be beneficial or not.

6. References

[1] D. Paladino, M. Andreani, R. Zboray and J. Dreier, "Toward a CFD-quality database addressing LWR containment phenomena", Proceedings of the OECD/NEA/IAEA Workshop on Experimental Validation and Application of CFD and CMFD codes to Nuclear Reactor Safety Issues (CFD4NRS-3), Washington D.C., USA, 2010, September 14-16.

[2] J. Vendel, J. Malet, A. Bentaib, H.J. Allelein, S. Schwarz, E. Studer, H. Paillère, K. Fischer, M. Houkema and ISP-47 participants "Conclusions of the ISP-47 - Containment Thermal-Hydraulics", Proceedings of the 12th International Topical Meeting on Nuclear Reactor Thermal-Hydraulics (NURETH-12, Log Number: 031, Pittsburgh, PA, USA, 2007, September 30 – October 4.

[3] E. Studer, J. Brinster, I, Tkatschenko, G. Mignot, D. Paladino and M. Andreani, "Interaction of a light gas stratified layer with an air jet coming from below: large scale experiments and scaling issues", Proceedings of the OECD/NEA/IAEA Workshop on Experimental Validation and Application of CFD and CMFD codes to Nuclear Reactor Safety Issues (CFD4NRS-3), Washington D.C., USA, 2010, September 14-16.

[4] D. Paladino, M. Huggenberger, M. Andreani, S. Gupta, S. Guentay, J. Dreier and H.M. Prasser, "LWR Containment Safety Research in PANDA", Proceedings of the 2008 International Congress on Advances in Nuclear Power Plants (ICAPP `08), Paper 8303, Anaheim, CA, USA, 2008, June 8-12.

[5] GOTHIC Containment Analysis Package, Version 7.2b (QA), EPRI, Palo Alto, CA, March 2009.

[6] M. Andreani, R. Kapulla and R. Zboray, "Simulation of Break-up of Gas Stratification by a Vertical Jet using the GOTHIC Code", Proceedings of the 8th International Topical Meeting on Nuclear Thermal-Hydraulics, Operation and Safety (NUTHOS-8), Paper N8P0340., Shanghai, China, 2010, October 10-14.

[7] J. Brinster, M. Cazanou, I. Tkatschenko and J.L. Widloecher "OECD SETH-2 project, Description of MISTRA facility SETH2-MISTRA-2008-12/a", CEA technical report, SFME/LEEF/RT/08-009/A, March 2009.

[8] D. Paladino, G. Mignot, R. Zboray, M. Fehlmann and H.J. Strassberger, "OECD SETH-II Project, PANDA test facility, description and geometrical specifications", PSI technical report, TM-42-08-07-0, September 2008.

[9] FLUENT Inc., "FLUENT 6.3 user's guide". FLUENT Inc., Lebanon, NH, 2006.

[10] B.E. Launder and D.B. Spalding, "Lectures in mathematical models of turbulence", Academic Press, London, England, 1972.

[11] V. Yakhot and S. A. Orszag, "Renormalization group analysis of turbulence: I. basic theory", Journal of Scientific Computing, 1(1), pp.1:51, 1986.

[12] S.V. Patankar, "Numerical heat transfer and fluid flow", Hemisphere, Washington, DC, 1980.

[13] R.I. Issa, "Solution of implicitly discretized fluid flow equations by operator splitting", J. Comput. Phys., Vol. 62, pp. 40-65. 1986

[14] M. Andreani and D. Paladino, "Simulation of gas mixing and transport in a multi-compartment geometry using the GOTHIC containment code and relatively coarse meshes", Nuclear Eng. Design, 240, pp. 1506-1527, 2010.

[15] N.Z. Ince and B.E. Launder, "Three-dimensional and heat-loss effects on turbulent flow in a nominally two-dimensional cavity", Int. J. Heat Fluid Flow, Vol. 16, pp. 171-177, 1995.